Multiple phase control in Mg through the continuum

A. Lyras[1] and H. Bachau[2]
[1]*Atomic and Molecular Physics Laboratory, Department of Physics, University of Ioannina, GR-45110 Ioannina, Greece*
[2]*Centre Lasers Intenses et Applications (CNRS—Université de Bordeaux I), Université de Bordeaux I, 351 Cours de la Libération, F-33405 Talence, France*
(Received 22 March 1999)

We present results from perturbative calculations on a scheme of coherent control in Mg. The scheme involves the excitation of Mg in the vicinity of an autoionizing resonance lying above the first two ionization thresholds by a two-color field composed of a fundamental frequency and its third harmonic, whose relative phase can be continuously controlled. Four as well as two-photon coherent excitation pathways, involving appropriate combinations of the two frequencies, proceed through the atomic continuum simultaneously contributing to the excitation, while three-photon ionization by the fundamental is also energetically possible. As a result, some of the excitation processes involve above-threshold ionization (ATI). The calculated ionization yields for the various groups of photoelectrons reveal significant modulation as the relative phase of the field component frequencies is varied. The modulation patterns for the different photoelectron groups are mutually shifted due to the multiphoton matrix element phases associated both with the ATI process and the multichannel nature of the final state. The effect is particularly pronounced when the autoionizing state is in near four-photon resonance with the fundamental frequency. The role of an autoionizing state as a final state as well as that of the continuum as an intermediate state in coherent control processes is discussed.
[S1050-2947(99)07712-4]

PACS number(s): 32.80.Rm, 42.50.Hz

The control of atomic and molecular response to laser field excitation has received considerable attention in the last decade. In particular, control of ionization, or dissociation by quantum-mechanical interference of excitation pathways that lead to the same final state, has been studied extensively both in experiment and in theory. In this context, an approach followed by many researchers is to excite the system with a bichromatic field whose component frequencies (usually a fundamental ω, and its third harmonic 3ω) have a well-defined and continuously adjustable phase difference. This approach is often called phase control, to emphasize the crucial role of the relative phase of the fields in controlling the system response, and to distinguish it from other coherent control mechanisms that are independent of field phases. Many atomic and molecular systems have been studied. Total as well as energy-, mass-, or angle-resolved products have been controlled (or shown to be controllable) in an efficient way [1–10].

In a recent experiment it was shown that a virtual state may replace the often used bound intermediate states in (ω, 3ω) phase-control schemes [8], and efficient control of four-photon resonant five-photon ionization was demonstrated. Another significant recent development, that prompted wide discussion in the literature, was the discovery of a phase lag in the modulation patterns of different, phase-controlled molecular ionization-dissociation products [10]. Formal derivations and model calculations were employed to interpret the origin of the observed phase lag [9–13], and it was concluded that the origin is related to a system-dependent phase that may vary according to the excitation scheme employed [10,11,13]. However, this interpretation is not unanimous [9,12]. The most recent experimental findings [14] provide further evidence as to the origin of the phase lag, the conditions under which it may be observed, and its importance for phase-control processes.

The motivation for our study stems from these developments, and has a twofold aim. First, we wish to explore the atomic continuum as an intermediate state in phase control schemes, thus expanding the part of the atomic spectrum amenable to phase control. Second, we wish to provide a reliable calculation of modulation patterns of different products, resulting from the phase control of ionization in a real system, subjective to experimental scrutiny. The identification of the origin of a phase lag in the modulation patterns would be facilitated in the context of such a calculation.

We have chosen to study Mg not only because theoretical results of sufficient accuracy can be obtained by a well-established approach, but also because it is a system well adapted to experimental work. The scheme we have chosen to investigate is shown in Fig. 1. A $^1D^e$ autoionizing (AI) resonance, lying above the $3p$ ionization threshold, is excited by a bichromatic (ω, 3ω) field. There are no resonances with bound states below the $3s$ ionization threshold or AI states between the $3s$ and $3p$ thresholds. This condition con-

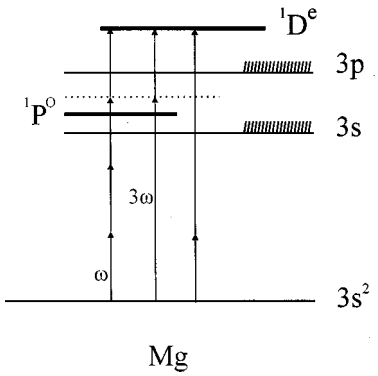

FIG. 1. Energy-level diagram for phase control in Mg.

siderably restricts the energy position of the final state, but other than that the choice of the final state is dictated by angular momentum selection rules only. To lowest nonvanishing order in perturbation theory, only three processes (schematically depicted in Fig. 1) contribute to its excitation. When the corresponding three amplitudes are of comparable strength, quantum interference effects would determine the excitation rate of the resonance and its autoionization decay. The interference could be controlled by varying the relative phase of the two component fields [3,9], and as a result the decay of the AI state to the $3s$ and $3d$ thresholds could be modulated. This modulation could be conveniently recorded in energy-resolved photoelectron spectra. A third group of photoelectrons would be produced by three- and one-photon absorption from the ground state with frequencies $\omega_1 \equiv \omega$ and $\omega_3 \equiv 3\omega$, respectively (Fig. 1). This ionization product would be also modulated, as the relative field phase would be varied, because of the quantum interference of the two pathways leading to its production (Fig. 1). These photoelectrons could also be separately recorded in energy-resolved photoelectron spectra, since their energy is quite different from that of the other two photoelectron groups.

We have evaluated all the parameters pertaining to the atomic levels coupled by the processes depicted in Fig. 1, by a procedure presented in detail in an earlier publication [15]. Here we repeat only the main steps of this approach. The Mg^{2+} ($1s^2 2s^2 2p^6$) core is represented by a self-consistent-field wave function. For the valence electrons we have applied a frozen-core approximation supplemented by a polarization potential that includes a dielectronic term [16]. One-electron orbitals are obtained by diagonalizing the Hamiltonian associated to Mg^+ on a basis of B-spline functions [17] that are orthonormalized to the Hartree-Fock core wave function. Two-electron configurations are constructed from antisymmetrized products of one-electron orbitals. Practically, we used a basis set of 350 B splines defined in a box 150 a.u. long. We used 400–600 two-electron configurations per angular momentum symmetry for $L \leqslant 4$, assuming LS coupling to be adequate for Mg in the studied energy range. We show results pertaining to the present study in Table I. The results compare well with the data published by Mengali and Moccia [18]. Our result for the ground-state energy is -0.8319 a.u. compared to -0.8336 a.u. for the experimental value; in the multiphoton calculations described in the following we have used the experimental value for the ground-state energy.

In Mg, a two-electron atom, the calculation of the multiphoton amplitudes for the processes shown in Fig. 1 is a nontrivial task, especially for high-order processes (order 3 or higher). The three amplitudes can be formally defined as

$$M^{(4)} = \langle f | D_1 G_3^{(+)} D_1 G_2^{(+)} D_1 G_1^{(+)} D_1 | in \rangle,$$

$$M_{13}^{(2)} = \langle f | D_3 G_1^{(+)} D_1 | in \rangle, \quad M_{31}^{(2)} = \langle f | D_1 G_3^{(+)} D_3 | in \rangle,$$

where $|in\rangle$ and $|f\rangle$ are, the initial and final states of the transition, respectively, that may be either the same or different depending on the selection rules that apply. D_j, $j=1$ and 3, are the dipole moment transition operators corresponding to the fundamental and the thrid-harmonic, respectively. Finally, the Green's operators are defined as

TABLE I. Energies, partial widths, and total width (all in a.u.) for three Al states of Mg (see text for details). Numbers in brackets represent powers of 10. For the conversion of units in the case of $3p4s$ we used for the ionization potential $Mg^+(3s)$ the values 15.035 eV and 1 a.u.=27.21 eV.

State	Energy (a.u.)	Partial width (a.u)		Total width (a.u.)
$^1P^o(3p4s)$	-0.4768	$3skp$	1.404 [−2]	1.40 [−2]
	-0.4751*			1.19 [−2]*
$^1S^e(4s^2)$	-0.3549	$3sks$	2.104 [−3]	6.06 [−3]
	-0.3556*	$3pkp$	3.959 [−3]	6.00 [−3]*
		$3skd$	5.024 [−3]	
$^1D^e(3d4s)$	-0.3317	$3pkp$	6.619 [−3]	1.35 [−2]
	-0.3303*	$3pkf$	1.844 [−3]	1.20 [−2]*

*Values calculated by Mengali and Moccia [J. Phys. B **29**, 1597 (1996)].

$$G_j^{(+)} = (E_{\text{in}} + j\omega_1 - H + i\varepsilon)^{-1}, \quad j = 1,\ 2,\ \text{and}\ 3.$$

In the present case the calculation is further complicated by the fact that in two of the amplitudes, namely, $M^{(4)}$ and $M_{31}^{(2)}$, the last step in the excitation involves a continuum-continuum transition (above-threshold ionization, ATI). Moreover, the final AI resonance decays into a multichannel continuum. We have employed an approach already applied to the study of two-photon absorption in H^-, He, and Be [19,20]. The approach has been generalized and efficiently implemented for three- and four-photon absorption with ATI, although in its present form it is computationally more involved. When the final state is close to an AI resonance, the Feshbach formalism [21] may be used to describe it. In this case the resonance parameters (position, width, etc.) may be extracted computationally. The amplitudes associated with the multiphoton couplings are calculated in the velocity gauge which is known to converge more rapidly [19,20]. We have considered three-photon ionization to channels $^1P^o$ and $^1F^o$, as well as four-photon ionization to channels $^1S^e$, $^1D^e$, and $^1G^e$. Channels such as $^1F^o$ and $^1G^e$ contribute only as background in the corresponding processes, and their importance is small when the interference takes place in the vicinity of a resonance. They become more important if one studies phase-controlled interference far from any final-state resonance. We have checked the numerical convergence of our multiphoton calculations in the usual way, i.e., by varying the number of states in the basis set and/or the box length. In general, good convergence has been obtained for total multiphoton ionization (MI) cross sections. However, we have found that some partial MI cross sections may still vary by 20%, even with a basis size increased up to the machine capacity limit. This may be the result of numerical problems, e.g., numerical cancellation effects, and as a consequence it becomes extremely difficult to obtain a highly accurate value. Nevertheless, we believe that the degree of accuracy reached in our calculations is sufficient for the purpose of the present work.

The ionization rate can be calculated by summing coherently the amplitudes of all three processes depicted in Fig. 1,

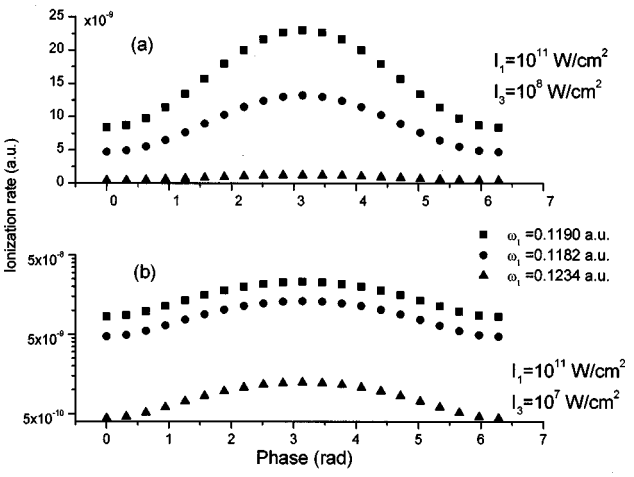

FIG. 2. Ionization rate (in a.u.) vs the relative field phase (δ in rad) for simultaneous three- and one-photon ionization from Mg($3s^2$). Details are shown on the plot.

i.e., first summing the amplitudes and then squaring the absolute value of the sum. In this way, one can obtain either the total ionization rate or partial ones. The latter will give the rate of production of a specific group of photoelectrons and the corresponding ions. However, we will start with a simpler and much studied case, on which there is still discussion in the literature. We will denote by E_1 the group of photoelectrons resulting from the simultaneous three- and one-photon ionization (by ω_1 and ω_3, respectively) above the $3s$ threshold. Their energy (in atomic units) is $E_1 = E_g + 3\omega_1 - E_{3s}$, where E_g is the ground-state energy, E_{3s} the energy of the $3s$ ionization threshold, and ω_1 the frequency of the fundamental (Fig. 1). We have ignored the ponderomotive shift of the ionization potential and ac Stark shift of the ground state, but we will comment on this point at the end of the paper. The corresponding ionization rate would result from the coherent summation of only two matrix elements, a one-photon matrix element and a three-photon one. The final expression could be written as

$$R_1 = 2\pi\{|M_f^{(3)}|^2 I_1^3 + |M_p^{(3)}|^2 I_1^3 + |M_p^{(1)}|^2 I_3 + 2|M_p^{(3)}||M_p^{(1)}| I_3^{1/2} I_1^{3/2} \cos(\delta + \delta_3 - \delta_1)\} \quad (1)$$

where $M_p^{(3)} = |M_p^{(3)}|\exp(i\delta_3)$ and $M_p^{(1)} = |M_p^{(1)}|\exp(i\delta_1)$ are the three- and one-photon amplitudes to the $^1P^o$ final-state symmetry, that interfere, and $M_f^{(3)}$ the corresponding amplitude to the $^1F^o$ final state that contributes to the signal background. The intensities of the two components of the bichromatic field are I_1 and I_3, respectively, and θ_1 and θ_3 are the corresponding field phases. The quantity $\delta = 3\theta_1 - \theta_3$ is assumed to be continuously variable in the interval $[0, 2\pi]$, a condition that is easily realized experimentally [2,8]. In Eq. (1), with the matrix elements expressed in atomic units (a.u.) and the intensities expressed in units of $I_0 = 1.4 \times 10^{17}$ W cm^{-2}, the rate R_1 is given in a.u., Some of the results obtained by applying Eq. (1) are shown in Fig. 2. Specifically, we have plotted the absolute value of the photoelectron production rate (in a.u.) as a function of δ for three different frequencies of the fundamental and for two combinations of fundamental and harmonic power densities. For $\omega_1 = 0.1190$ a.u. the three-photon final state is $^1P^o(3p4s)$, while for the other two frequencies no bound or AI resonance is met in the excitation-ionization process. From the plotted results we observe that for a certain choice of fundamental and harmonic power densities the modulation of the signal can be enhanced near a suitably chosen resonance [Fig. 2(a)], while for other combinations of power densities the off-resonant signal may have an equally significant modulation to that of the on-resonant one [Fig. 2(b)]. Of course, near a resonance the magnitude of the ionization signal is always significantly enhanced. For example, at $\omega_1 = 0.1182$ a.u. the three-photon energy is detuned from the center of the AI resonance but lies within its broad width. As a result, the modulation patterns for the two frequencies exhibit very similar dependence on the power density although the absolute value of the yield is, of course, different, being significantly enhanced close to the center of the resonance. The behavior for $\omega_1 = 0.1234$ a.u. is noticeably different, since for this frequency there is no influence of the $^1P^o$ resonance (or any other) on the final state. By analyzing the photoelectron yield vs harmonic intensity, for fixed frequency and intensity of the fundamental, one may find various combinations of parameters resulting in efficient control. For $I_1 = 10^{11}$ W cm^{-2}, efficient control is obtained with $I_3 = 10^7 - 10^8$ W cm^{-2}. Although the latter values are certainly realistic, other combinations can be found, but an exhaustive search is meaningful only when a specific experiment is planned.

In all cases studied on, near, or far from the final-state resonance the modulation patterns were in phase and no phase lag was obtained. This conclusion is in line with earlier [3,9] and recent [12,13] theoretical results, and the most recent experimental data [10,14]. This behavior results from the fact that $\delta_1 = \delta_3$ in Eq. (1), whenever there is a single ionization channel (for a given final-state total angular momentum L) affected by interference ($^1P^o$ in the present case) and there is no ATI contributing to the ionization.

We now continue with the presentation of the results pertaining to the full excitation scheme as depicted in Fig. 1. Two new groups of photoelectrons (in addition to E_1) are produced. They are denoted by E_2 and E_3, and their energies are $E_2 = E_g + 4\omega_1 - E_{3s}$ and $E_3 = E_g + 4\omega_1 - E_{3p}$, respectively. The expressions for the corresponding rates are more complicated than Eq. (1), since the number of channels is increased as a result of the higher order of the interfering processes. Specifically, for the E_2 group the interference affects the $3s\varepsilon s\ ^1S^e$ and $3s\varepsilon d\ ^1D^e$ channels, while the $3s\varepsilon g\ ^1G^e$ remains unaffected. Near the $^1D^e$ resonance, the importance of channels of different symmetry is reduced. However, we will examine off-resonant excitation as well, and including all significantly contributing channels is important. The expression for the photoelectron production rate can be written as

$$R_2 = 2\pi(R_{2,\text{incoh}} + R_{2,\text{coh}}),$$

where $R_{2,\text{incoh}}$ contains the terms unaffected by the interference, and $R_{2,\text{coh}}$ is subject to periodic modulation by the externally controlled relative phase of the fields. The two components are given by the following expressions:

$$R_{2,\mathrm{incoh}}=|\tilde{M}_g^{(4)}|^2I_1^4+|\tilde{M}_s^{(4)}|^2I_1^4+|\tilde{M}_d^{(4)}|^2I_1^4 +\{|\tilde{M}_{s,13}^{(2)}|^2+|\tilde{M}_{s,31}^{(2)}|^2+|\tilde{M}_{d,13}^{(2)}|^2 +|\tilde{M}_{d,31}^{(2)}|^2+2|\tilde{M}_{d,13}^{(2)}||\tilde{M}_{d,31}^{(2)}|\cos(\tilde{\delta}_{d,13}^{(2)}-\tilde{\delta}_{d,31}^{(2)}) +2|\tilde{M}_{s,13}^{(2)}||\tilde{M}_{s,31}^{(2)}|\cos(\tilde{\delta}_{s,13}^{(2)}-\tilde{\delta}_{s,31}^{(2)})\}I_1I_3, \quad (2)$$

$$R_{2,\mathrm{coh}}=2|\tilde{M}_d^{(4)}|I_1^{5/2}I_3^{1/2}\{|\tilde{M}_{d,13}^{(2)}|\cos(\delta+\tilde{\delta}_d^{(4)}-\tilde{\delta}_{d,13}^{(2)}) +|\tilde{M}_{d,31}^{(2)}|\cos(\delta+\tilde{\delta}_d^{(4)}-\tilde{\delta}_{d,31}^{(2)})\} +2|\tilde{M}_s^{(4)}|I_1^{5/2}I_3^{1/2}\{|\tilde{M}_{s,13}^{(2)}|\cos(\delta+\tilde{\delta}_s^{(4)}-\tilde{\delta}_{s,13}^{(2)}) +|\tilde{M}_{s,31}^{(2)}|\cos(\delta+\tilde{\delta}_s^{(4)}-\tilde{\delta}_{s,31}^{(2)})\}, \quad (3)$$

where $\tilde{M}_d^{(4)}=|\tilde{M}_d^{(4)}|\exp(i\tilde{\delta}_d^{(4)})$ and $\tilde{M}_s^{(4)}=|\tilde{M}_s^{(4)}|\exp(i\tilde{\delta}_s^{(4)})$ are the four-photon matrix elements to the $^1D^e$ and $^1S^e$ final-state channels, respectively. The two-photon matrix elements should be distinguished according to the process they represent. Therefore, $\tilde{M}_{d,13}^{(2)}=|\tilde{M}_d^{(2)}|\exp(i\tilde{\delta}_{d,13}^{(2)})$ and $\tilde{M}_{d,31}^{(2)}=|\tilde{M}_d^{(2)}|\exp(i\tilde{\delta}_{d,31}^{(2)})$ are the two-photon matrix elements to the $^1D^e$ final-state channel corresponding, respectively, to $(\omega_1+\omega_3)$ and $(\omega_3+\omega_1)$ excitation. The latter process involves an ATI step in the two-photon excitation and is, therefore, qualitatively different from the former. The corresponding matrix elements to the $^1S^e$ final-state channel are $\tilde{M}_{s,13}^{(2)}=|\tilde{M}_s^{(2)}|\exp(i\tilde{\delta}_{s,13}^{(2)})$ and $\tilde{M}_{s,31}^{(2)}=|\tilde{M}_s^{(2)}|\exp(i\tilde{\delta}_{s,31}^{(2)})$. All other symbols and the units have the same definition as in Eq. (1). Formally similar but far more complicated expressions can be given for the production rate of the E_3 photoelectrons. Partitioning the rate in two components,

$$R_3=2\pi(R_{3,\mathrm{incoh}}+R_{3,\mathrm{coh}}),$$

we have

$$R_{3,\mathrm{incoh}}=|M_g^{(4)}|^2I_1^4+|M_s^{(4)}|^2I_1^4+\{|M_{s,13}^{(2)}|^2+|M_{s,31}^{(2)}|^2 +2|M_{s,13}^{(2)}||M_{s,31}^{(2)}|\cos(\delta_{s,13}^{(2)}-\delta_{s,31}^{(2)})\}I_1I_3 +\sum_{i=1}^{2}[|M_d^{i,(4)}|^2I_1^4+\{|M_{d,13}^{i,(2)}|^2+|M_{d,31}^{i,(2)}|^2 +2|M_{d,13}^{i,(2)}||M_{d,31}^{i,(2)}|\cos(\delta_{d,13}^{i,(2)}-\delta_{d,31}^{i,(2)})\}I_1I_3], \quad (4)$$

$$R_{3,\mathrm{coh}}=2\sum_{i=1}^{2}|M_d^{i,(4)}|I_1^{5/2}I_3^{1/2}\{|M_{d,13}^{i,(2)}|\cos(\delta+\delta_d^{i,(4)}-\delta_{d,13}^{i,(2)}) +|M_{d,31}^{i,(2)}|\cos(\delta+\delta_d^{i,(4)}-\delta_{d,31}^{i,(2)})\} +2|M_s^{(4)}|I_1^{5/2}I_3^{1/2}\{|M_{s,13}^{(2)}|\cos(\delta+\delta_s^{(4)}-\delta_{s,13}^{(2)}) +|M_{s,31}^{(2)}|\cos(\delta+\delta_s^{(4)}-\delta_{s,31}^{(2)})\}. \quad (5)$$

Additional notation has been introduced in Eqs. (4) and (5) to take into account the fact that when the ion is left in the $Mg^+(3p)$ state the available final-state channels are increased. Specifically, there is only one $^1S^e$ channel, namely, $3p\varepsilon p$, but two of $^1D^e$ symmetry, namely, $3p\varepsilon p$ and $3p\varepsilon f$.

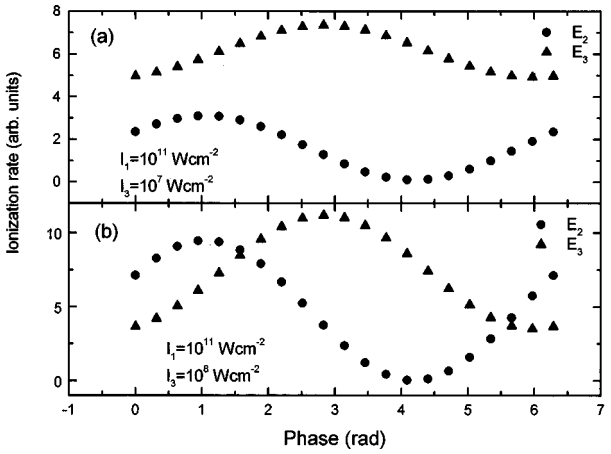

FIG. 3. Ionization rates (in arbitrary units) vs the relative field phase (δ in rad) for simultaneous four-and two-photon ionization from $Mg(3s^2)$. The fundamental photon frequency is 0.1255 a.u., resonantly exciting the $^1D^e(3d4s)$.

Therefore, we introduce an additional superscript i that takes the values 1 and 2 for the $3p\varepsilon p$ and $3p\varepsilon f$ channels, respectively. Typical examples are the four-photon matrix element $M_d^{1,(4)}=|M_d^{1,(4)}|\exp(i\delta_d^{1,(4)})$ to the $3p\varepsilon p$ channel or the two-photon matrix element $M_{d,13}^{2,(2)}=|M_{d,13}^{2,(2)}|\exp(i\delta_{d,13}^{2,(2)})$ to the $3p\varepsilon f$ channel corresponding to the process $(\omega_1+\omega_3)$. Coherent summation over this new index is required in order to describe the interference process correctly and is, indeed, shown in Eqs. (4) and (5). An incoherent summation over the final-state channels of G symmetry has been suppressed in Eq. (4) in order to save space and simplify the notation.

A representative collection of the results we obtained by appropriately applying formulas (2)–(5) is plotted in Figs. 3–5. To resonantly excite by four-photon absorption the $^1D^e$ resonance included in Table I, the fundamental frequency should be $\omega_1=0.1255$ a.u. It should be mentioned that as the number of absorbed photons is increased, in order to probe highly excited parts of the atomic spectrum, it increases accordingly the chance for accidental and unwanted intermediate resonances. A pertinent example is the four-photon excitation of the $^1S^e(4s^2)$ resonance (Table I). The fundamental

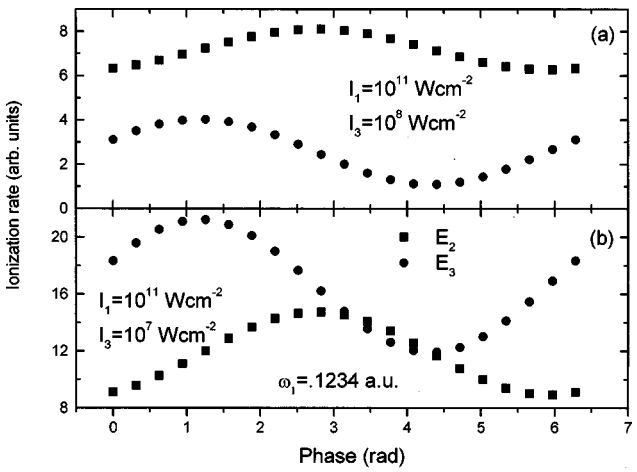

FIG. 4. Ionization rates (in arbitrary units) vs the relative field phase (δ in rad) for simultaneous four-and two-photon ionization from $Mg(3s^2)$. Details are shown on the plot.

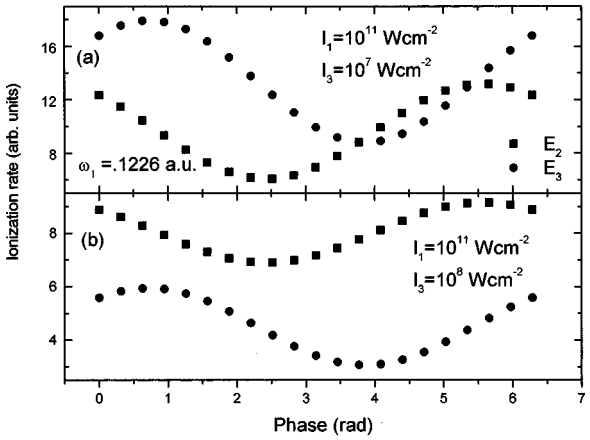

FIG. 5. Ionization rates (in arbitrary units) vs the relative field phase (δ in rad) for simultaneous four-and two-photon ionization from Mg($3s^2$). Details are shown in the plot.

frequency should be $\omega_1=0.1190$ a.u., and a three-photon resonance with the $^1P^e(3p4s)$ occurs. This may not necessarily be a drawback as far as phase control is concerned. However, a perturbative treatment, like the one employed in the present work, is not sufficient for a description of this doubly resonant excitation-control scheme. A time-dependent treatment in the framework of the density-matrix formalism, including all resonant states, should be employed. Additional parameters, such as the pulse duration and the temporal overlap of the fundamental and harmonic pulses, will also determine the outcome of the control process. Therefore, this is quite a different control scheme that will be presented in a separate, future publication.

In Fig. 3 we present two sets of results obtained for $\omega_1=0.1255$ a.u. for two combinations of fundamental and harmonic power densities. The absolute value of these ionization rates is approximately two orders of magnitude lower compared to the ones for the (ω,3ω) scheme shown in Fig. 2. The absolute values of the rates drawn in parts (a) and (b) of Fig. 3 are of the same order of magnitude, but cannot be compared directly because different scaling has been employed in each part, in order to make the modulation clearly visible. Within each part comparison of relative magnitudes is, of course, meaningful. We observe that substantial modulation is possible for both groups of photoelectrons for the appropriate combination of the fundamental and harmonic power densities. It is a useful reminder to experimentalists that not too high harmonic power densities actually enhance the signal modulation or, equivalently, increase the degree of control, as is evident by comparing Figs. 3(b) and 3(a). It is also evident that the relative yield of the two products would change as the power densities of the two field components are varied. In a certain sense, this is also a control mechanism of the relative photoelectron yield. However, it lacks the continuous variation and the periodicity that the phase-dependent mechanism exhibits, affording greater flexibility for control. In these plots we have not included the background contribution of the $^1G^e$-final-state channels in order to point out that the modulation of the E_2 signal goes through very low values, practically reaching zero. Although we have a multichannel final state, the modulation of the E_2 signal is mainly determined by interference in *one* $^1D^e$-final-state channel, that is dominant because of the resonant AI state, and to a far lesser degree by interference in *one* $^1S^e$ channel. The result is the almost perfect cancellation of the ionization rate for the E_2 photoelectrons. In an experiment, the background contribution will fill this deep modulation minimum, but it would still be much deeper compared to the minima of the E_3 signal. The most conspicuous feature of the results is the phase lag of the modulation patterns of the two products, i.e., the phase difference of signal maxima for a given fundamental wavelength and a specific combination of fundamental and harmonic power densities. We have found that the E_2 maximum lags the E_3 maximum by 0.6π rad or 108° [Fig. 3(b)]. Moreover, if one takes into account that the modulation pattern for the E_1 photoelectrons at $\omega_1=0.1255$ a.u. agrees with the one shown in Fig. 2, then all three ionization products are modulated out of phase with the E_2 peak lagging 108° behind the E_3 peak which, in turn, lags 18° behind the E_1 peak. It is worth mentioning that at this fundamental frequency the E_1 photoelectrons exhibit a modulation depth of approximately 2% i.e., rather insignificant compared to the modulation depth of the E_2 and E_3 photoelectrons in Fig. 3(b). Note that, as suggested by formulas (2)–(5), there is no intensity dependence of the phase lag, within the limits of our lowest nonvanishing order perturbative approach and the range of power densities we investigated, i.e., 10^9 W cm$^{-2}\leqslant I_1\leqslant 10^{11}$ W cm^{-2} and 10^5 W cm$^{-2}\leqslant I_3\leqslant 10^8$ W cm^{-2}.

In an effort to investigate the wavelength dependence of the phase lag as well as the effect of the final-state resonance on the degree of control, we have employed two other fundamental frequencies in our calculations. For $\omega_1=0.1234$ a.u., the final-state energy lies well outside the width of the broad $^1D^e$ resonance we have considered so far. The results are shown in Fig. 4. The absolute value of the rates is reduced compared to that obtained on resonance with the $^1D^e$ resonance, but the phase modulation of the rates is of the same magnitude [compare Figs. 3(a) and 4(b)]. Therefore, the phase control is efficient even far from the final-state resonance. The phase lag of the products is appreciably different compared to Fig. 3. The E_3 peak lags behind the E_2 peak by $\pi/2$ or 90°. To further test the wavelength dependence we have calculated the same quantities for $\omega_1=0.1226$ a.u., i.e., further detuned from resonance. The results are presented in Fig. 5. It is confirmed that coherent control is still possible away from the resonance. Comparing Figs. 5(a) and 4(b), we observe that the modulation depth may be even enhanced away from resonance. A phase lag in the modulation patterns of the two products is again evident. If one chooses to define the lag as the phase difference between signal maxima lying on the same side with respect to π (as we have done in the two cases examined earlier), then it is found that E_2 lags behind the E_3 by approximately 82°. It is very difficult from expressions (2)–(5) to identify unambiguously the source of the phase lag. However, it is worth noting that the phases of the interfering matrix elements have a qualitatively different behavior as a function of the fundamental photon frequency. This is in agreement with Refs. [11] and [13], where it was pointed out that ATI and coupled final-state channels, as met above the $Mg^+(3p)$ threshold, lead to photon-frequency-dependent phase lag. More specifically, the two matrix elements that correspond to

processes including an ATI step show substantial variation of their phase as a function of photon frequency, while for the remaining one the phase varies very slowly as the fundamental frequency is reduced from 0.1255 to 0.1226 a.u. We are therefore led to the conclusion that in our system and for the specific excitation scheme the variation of the phase lag by tuning the fundamental photon frequency is mainly due to the ATI process [11], and the channel coupling in the final-state resonance is less crucial. However, it may be useful to remind the reader that it is not possible to disentangle the contribution of the ATI process to the matrix element phase from the contribution of the final-state AI resonance. A qualitative comparison of our results with the experimental data presented in Refs. [10,14] should take into account the fact that the $^1D^e$ is a broad resonance, and detuning in its immediate vicinity is not meaningful. We have therefore detuned far outside its AI width to study the wavelength dependence of the modulation patterns and their phase lag. Moreover, there is no continuum-continuum transition involved in their excitation scheme. Nevertheless, a qualitative feature of their data, namely, a gradual decrease of the phase lag away from resonance [14], is met in our results as well. Comparing our numerical results with predictions from model calculations [11] or formal derivations [13] we obtain, in general, qualitative agreement as to the possible origin of a phase lag in the modulation patterns of the controlled products.

In conclusion, we have confirmed by a full perturbative calculation in a correlated two-electron system (Mg) that phase control of ionization by interfering three- and one-photon transitions to a single continuum channel may lead to significant modulation either near or far from an excited resonance. The presence of the resonance may enhance the overall ionization but not necessarily the modulation depth. It is clear that the fundamental and harmonic power densities should be chosen so that the contribution of the interference-induced cross terms balances the contribution corresponding to the direct ones in order to obtain maximum modulation or equivalently most efficient control. The modulation patterns near or far from resonance are in phase; no phase lag was obtained. We have also studied the control potential of four- and two-photon interfering excitations near or far from appropriate Al states, in a scheme that involved the continuum spectrum as an intermediate state. We have obtained significant modulation of the energy-resolved ionization products both near and far from resonance. The modulation patterns of the products exhibit a frequency-dependent phase lag that results from the particular excitation scheme employed in the specific system. This seems to be a ubiquitous feature in all multichannel phase-control schemes. Moreover, our findings seem to suggest that it may be possible by appropriately tuning the fundamental frequency to arrange for the maximum of the modulation pattern of one product to coincide with the minimum of the other. Of course, such a possibility, if experimentally confirmed, it would be far more important for molecular systems than for atomic ones.

Immediate extension of the present work has already been discussed in the text. We would like to point out that the explicit time dependence, inevitable in an experimental test of our results, is missing from our perturbative approach. Although some details may indeed be different (e.g., the modulation depth) the general features should agree well. The use of high power densities for the fundamental is necessary since four-photon ATI processes are studied. At these intensities and wavelengths the ponderomotive shift of the ionization threshold is a few cm^{-1}, and it should not affect the results. The same applies for the ac Stark shift of the ground state. As is often the case in such studies, the ionization of the final-state AI resonance by the fundamental was neglected. It should not be very important for the intensities employed in our calculations given the broad AI width of the particular resonance. It is therefore deemed possible to expect an experimental verification of our results, if not in Mg, at least in some of the other alkaline-earth atoms under comparable conditions.

One of us (A.L.) would like to thank the Universitéde Bordeaux I for the hospitality and financial support at the initial stage of this work.

[1] M. Shapiro, J. M. Hepbum, and P. Brumer, Chem. Phys. Lett. **149**, 451 (1988).
[2] Ce Chen, Yin Yi-Yian, and D. S. Elliott, Phys. Rev. Lett. **64**, 507 (1990); Ce Chen and D. S. Elliott, *ibid.* **65**, 1737 (1990); Yin Yi-Yian, Ce Chen, and D. S. Elliott, *ibid.* **69**, 2353 (1992).
[3] T. Nakajima, P. Lambropoulos, S. Cavalieri, and M. Matera, Phys. Rev. A **46**, 7315 (1992); T. Nakajima and P. Lambropoulos, Phys. Rev. Lett. **70**, 1081 (1993); Phys. Rev. A **50**, 595 (1994).
[4] Zidang Chen, P. Brumer, and M. Shapiro, Chem. Phys. Lett. **198**, 498 (1992); J. Chem. Phys. **98**, 6843 (1993).
[5] A. D. Bandrauk, J. M. Gauthier, and J. F. McCann, Chem. Phys. Lett. **200**, 399 (1992).
[6] B. Sheehy, B. Walker, and L. F. DiMauro, Phys. Rev. Lett. **74**, 4799 (1995).
[7] S. Lu, S. M. Park, Y. Xie, and R. J. Gordon, J. Chem. Phys. **96**, 6613 (1992); R. J. Gordon, S. Lu, S. M. Park, K. Trentelman, Y. Xie, L. Zhu, A. Kumar, and W. J. Meath, *ibid.* **98**, 9481 (1993); L. Zhu, V. Kleiman, X. Li, S. Lu, K. Trentelman, and R. J. Gordon, Science **270**, 77 (1995).
[8] N. E. Karapanagioti, D. Xenakis, D. Charalambidis, and C. Fotakis, J. Phys. B **29**, 3599 (1996).
[9] T. Nakajima, J. Zhang, and P. Lambropoulos, J. Phys. B **30**, 1077 (1997).
[10] L. Zhu, K. Suto, J. A. Fiss, R. Wada, T. Seideman, and R. J. Gordon, Phys. Rev. Lett. **79**, 4108 (1997).
[11] S. Lee, J. Chem. Phys. **107**, 2734 (1997).
[12] H. Lefebvre-Brion, J. Chem. Phys. **106**, 2544 (1997).
[13] T. Seideman, J. Chem. Phys. **108**, 1915 (1998).
[14] J. A. Fiss, L. Zhu, R. J. Gordon, and T. Seiderman, Phys. Rev. Lett. **82**, 65 (1999).
[15] N. E. Karapanagioti, D. Charalambidis, C. J. G. J. Uiterwaal, C. Fotakis, H. Bachau, I. Sanchez, and E. Cormier, Phys. Rev. A **53**, 2587 (1996).
[16] R. Moccia and P. Spizzo, Phys. Rev. A **39**, 3855 (1989).

[17] C. de Boor, *A Practical Guide to Splines* (Springer, New York, 1978).
[18] S. Mengali and R. Moccia, J. Phys. B **29**, 1597 (1996).
[19] I. Sanchez, H. Bachau, and E. Cormier, J. Phys. B **28**, 2367 (1995).
[20] I. Sanchez, F. Martín, and H. Bachau, J. Phys. B **28**, 2863 (1995).
[21] H. Feshbach, Ann. Phys. (N.Y.) **19**, 287 (1962).